Heat Transfer Enhancement in Swirl Annulus Flows

ALI M. JAWARNEH
Department of Mechanical Engineering
The Hashemite University, Zarqa 13115, Jordan
E-mail: jawarneh@hu.edu.jo

Abstract: The characteristics of decaying swirling flows and forced convective heat transfer on the condition of turbulent flow in a narrow concentric annulus were simulated. The governing equations are solved numerically via a finite volume method. Uniform wall temperature at the inner wall and adiabatic wall at the outer wall are considered as thermal boundary conditions. Solutions for the axial and swirl velocity distributions and the Nusselt number are obtained for different values of the inlet swirl number and the Reynolds number. Simulations show that the inlet swirl number have great influences on the heat transfer characteristics. Under developed turbulent flow conditions, the increases of inlet swirl number will enhance the heat transfer. When the inlet swirl number increases it increases the axial velocity near the wall and reduces it at the mid-gap to achieve the conservation of mass due to the existence of secondary flows in the annulus due to centrifugal forces. The increase of the near-wall velocity, in turn, produces larger temperature gradients and higher heat transfer rate. The swirl velocity profiles decay gradually downstream as a result of friction which leads to damp the tangential velocity. The comparison between predicted and experimental data of average Nusselt numbers was found to be in good agreement.

Keywords: Swirl Flow; Nusselt Number; Turbulence; Narrow Annulus

1 Introduction

Forced convection in an annulus between two horizontal concentric cylinders has been investigated extensively in the literature [1-3] because of its wide variety of practical and technical applications such as heat exchangers. The production of small size and inexpensive but effective heat exchangers to transfer more heat from the surfaces of heat exchangers is a very important subject in heat transfer. Swirl flows are found in nature, such as tornadoes, and are utilized in a very wide range of applications, such as cyclone separators, agricultural spraying machines, heat exchangers, gasoline engines, diesel engines, gas turbines and many other practical heating devices [4]. A Swirl flow devices are designed to impart a rotational motion about an axis parallel to the flow direction to the bulk flow and is one of the passive enhancement techniques used for increasing the rate of heat transfer [5]. The use of decaying swirl flow is one of most promising techniques for enhancing the mass and heat transfer. The swirling effect to the fluid is given upstream section, and then allowed to decay along the length of a tube [6]. The presence of swirl will increase the flow path, decrease the free area and introduce an angular acceleration to the fluid flow [7]. Swirling flows can be imparted to the flow by use of various swirl-generating methods [8-10] where part of fluid enters axially while the reminder is injected tangentially using a vortex generator. Different swirl intensities can be achieved by varying the fluid flow rate at the axial and tangential inlets. Martemianov and Okulov [11] proposed theoretical model of the heat transfer in the axisymmetric swirl pipe flows. Their study shows that wake-like swirl flows will increase the heat transfer comparison with the axial flow while the jet-like swirl flows can diminish the heat transfer. Zeng et al [12] investigated the characteristics of the flow and convective heat transfer on the conditions of both developed laminar and turbulent flow in bilaterally heat narrow annuli. The convective heat transfer depends on the combination effect of the heat-flux ratio and the Reynolds number. Under laminar flow condition, the decreases of the gap size will lead to the heat transfer deterioration both on the inner and outer walls. However with respect to the case of the turbulent flow conditions, it is quite different. The decrease of the gap size will yield heat transfer deterioration on the inner wall, but it will enhance the heat transfer coefficient on the outer wall. Akpinar and Bicer [13] investigated the effect of swirl generator on heat transfer rates, swirl generator were placed at the entrance section of inner pipe of heat exchanger. Experiments were carried out for both parallel and counter flow models of the fluids at different Reynolds numbers. It was observed that the Nusselt number could increase up to 130% by giving rotation to the air with the help of the swirl elements. Several studies have indicated that helically coiled tubes are superior to straight tubes when employed in heat transfer applications [14-16]. The centrifugal force due to the curvature of the tube results in the development of secondary flows (flows perpendicular to the axial direction) which assist in mixing the fluid

and enhance the heat transfer. These situations can arise in the food processing industry for the heating and cooling of either highly viscous liquid food, such as pastes or purees, or for products that are sensitive to high shear stresses. Lu and Wang [17] have investigated experimentally the convection heat transfer characteristics of water flow in a narrow annulus without swirl. Experimental results show that the heat transfer characteristics of single-phase water flow in the narrow annulus are different from those in circular tubes. The transition from the laminar to turbulent heat transfer in the narrow annulus is earlier than that in circular tubes. When the Reynolds number is lower than 150, the heat transfer deteriorates, and the axial heat conduction has an important influence on the overall heat transfer. The transition from laminar to turbulent heat transfer is in the Reynolds number range from 800 to 1200. In the turbulent flow area, a narrow annulus can achieve the enhancement of heat transfer. Dirker and Meyer [18] conducted experiments of heat transfer coefficients at the inner wall of smooth concentric annuli for turbulent flow of water with wide range of diameter ratios and the Wilson plot technique was used to develop a convection heat transfer correlation. It was found the convection heat transfer correlation for an annulus was dependent on the annular diameter ratios. The deduced correlation predicted Nusselt numbers accurately within 3% of measured values for a Reynolds number range, based on the hydraulic diameter, from 4000 to 30,000. Ichimiya et al. [19] carried out experiments of forced convection heat transfer in a narrow concentric annulus by turbulence promoters to examine the effects of promoters. An experimental study of a double-pipe helical heat exchanger was performed using two differently sized heat exchangers has been experimentally done by [20]. Overall heat transfer coefficients were calculated and heat transfer coefficients in the inner tube and the annulus were determined using Wilson plots. The effect of swirl in axial flow through a narrow gap has been studied by [21]. The characteristics of turbulent swirling flow in an axisymmetric annuli using the PIV technique has been studied by [22]. Numerical study has been performed by [23] to estimate the hydrodynamics of an annular swirling decaying flow induced by means of a single tangential inlet in laminar flow regime. The mean swirl intensity in the whole annular gap thickness has been found to decrease from the entrance section.

The methodology of calculating the Nusselt number and velocity components in the annulus of the heat exchanger is quite incomplete in the open literature for decaying vortex flow. Therefore, this paper concerns a numerical study of turbulent flow of an incompressible viscous fluid confined between two stationary tubes with a small gap using a finite volume method. The main purpose in the present work is to show the effect of inlet swirl number on heat transfer in the form of Nusselt number for developed turbulent flow within the annulus.

2 Analysis

2.1 Governing Equations

Fig.1 shows the schematic of the annulus and co-ordinates system. The flow under study is steady, turbulent, incompressible and axisymmetric. The outer and inner radii of the concentric annulus are r_o and r_i, respectively. The fluid enters the cylinders gap uniformly with two velocity components (V, U) in z, θ directions, where V and U denote the axial and tangential inlet velocity components, respectively. The thermo physical properties of fluid are assumed constant except density for which the Boussinesq approximation is employed such that the variation of density with temperature has been neglected. The basic equations governing fluid flow and heat transfer in annular geometry are the laws of conservation of mass, momentum, energy, turbulent kinetic energy and its dissipation rate. The equations will be solved by assuming that the gap between the two cylinders is small, and the radial velocity is also assumed to be zero since it doesn't have the space and time to develop. The governing equations in the annulus are written as:

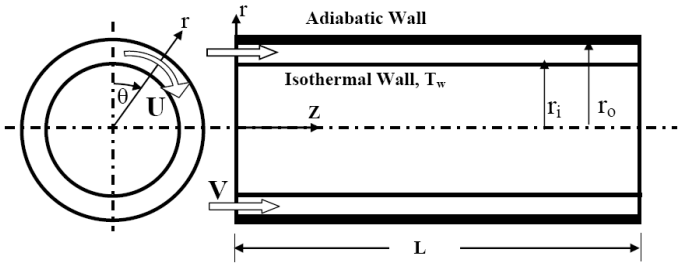

Fig.1: Swirling flow between two concentric cylinders

Continuity:

$$\frac{\partial}{\partial x_i}(\rho u_i) = 0 \tag{1}$$

Momentum:

$$\frac{\partial}{\partial x_j}(\rho u_i u_j) = -\frac{\partial p}{\partial x_i} + \frac{\partial}{\partial x_j}[\mu(\frac{\partial u_i}{\partial x_j} + \frac{\partial u_j}{\partial x_i} - \frac{2}{3}\delta_{ij}\frac{\partial u_l}{\partial x_l})] + \frac{\partial}{\partial x_j}(-\rho\,\overline{u_i' u_j'}) \tag{2}$$

Energy:

$$\frac{\partial}{\partial x_i}[u_i(\rho E + p)] = \frac{\partial}{\partial x_j}[k_{eff}\frac{\partial T}{\partial x_j} + u_i(\tau_{ij})_{eff}] \tag{3}$$

where E is the total energy and $(\tau_{ij})_{eff}$ represents the viscous heating, defined as

$$(\tau_{ij})_{eff} = \mu_{eff}(\frac{\partial u_j}{\partial x_i} + \frac{\partial u_i}{\partial x_j}) - \frac{2}{3}\mu_{eff}\frac{\partial u_i}{\partial x_i}\delta_{ij} \tag{4}$$

the effective thermal conductivity is

$$k_{eff} = \alpha C_p \mu_{eff} \tag{5}$$

The inverse effective Prandtl numbers, α, is set to be 1.393 for high Reynolds number. The renormalization group (RNG) $k-\varepsilon$ model is

similar in form to the standard $k-\varepsilon$ model, but it has shown considerable improvements over the standard $k-\varepsilon$ model where the flow features of strong streamline curvature, vortices, and rotation are included. Transport equations for the RNG $k-\varepsilon$ model are

$$\frac{\partial(\rho k u_i)}{\partial(x_i)} = \frac{\partial}{\partial(x_j)}(\alpha_k \mu_{eff} \frac{\partial k}{\partial x_j}) - \rho \overline{u_i' u_j'} \frac{\partial u_j}{\partial x_i} - \rho\varepsilon \quad (6)$$

$$\frac{\partial(\rho \varepsilon u_i)}{\partial(x_i)} = \frac{\partial}{\partial(x_j)}(\alpha_\varepsilon \mu_{eff} \frac{\partial \varepsilon}{\partial x_j}) + C_1 \frac{\varepsilon}{k}(\rho \overline{u_i' u_j'} \frac{\partial u_j}{\partial x_i}) - C_2 \rho \frac{\varepsilon^2}{k} + R_\varepsilon \quad (7)$$

The quantities α_k and α_ε are the inverse effective Prandtl numbers for k and ε and for high Reynolds number their values are $\alpha_k = \alpha_\varepsilon \approx 1.393$. The effective Viscosity μ_{eff} is the sum of the laminar μ and turbulent viscosities μ_t,

$$\mu_t = \rho C_\mu \frac{k^2}{\varepsilon} \quad (8)$$

The model constants; C_1, C_2 and C_μ are 1.42, 1.68 and 0.0845, respectively. The main difference between the RNG and standard $k-\varepsilon$ model lies in the additional term in the ε equation given by

$$R_\varepsilon = \frac{C_\mu \rho \eta^3 (1-\eta/\eta_0)}{1+\beta\eta^3} \frac{\varepsilon^2}{k} \quad (9)$$

where $\eta = S_n k/\varepsilon$, $\eta_0 = 4.38$, $\beta = 0.012$. The swirl number S_n is defined as the ratio of the axial flux of angular momentum to the axial flux of axial momentum: $S_n = \int_{r_i}^{r_o} \rho V_z V_\theta r^2 dr / (r_o - r_i) \int_{r_i}^{r_o} \rho V_z r^2 dr$ (10)

where V_z and V_θ denote the axial velocity and swirl velocity components. Turbulence is affected by the swirl in the mean flow. The RNG model provides an option to account for the effects of swirl by modifying the turbulent viscosity appropriately. The modification takes the following functional form,

$$\mu_t = \mu_{to} f(\Psi, S_n, \frac{k}{\varepsilon}) \quad (11)$$

where μ_{to} is the value of the turbulent viscosity calculated without the swirl modification using Eq.(8), and Ψ is a swirl constant that takes on different values depending on whether the flow is swirl-dominated or only mildly swirling. For strongly swirling flows as in the present work a value of 0.08 was used.

2.2 Materials and Boundary Conditions

Simulations have been done for different Reynolds numbers and different inlet swirl numbers. In the present simulations, the Reynolds number range, based on the annular hydraulic diameter $D_h = 2(r_o - r_i)$, of 5000–10000 is covered and the inlet swirl number range of 0-3 is covered. The Reynolds number Re and inlet swirl number S, which measures the ratio of the rate of the injected tangential momentum flux to the rate of axial momentum flux, are defined as

$$\mathrm{Re} = \frac{\rho V D_h}{\mu} \quad (12)$$

$$S = \frac{U}{V} \quad (13)$$

We define non-dimensional quantities as follows:

$$\bar{V_z} = \frac{V_z}{V},\ \bar{V_\theta} = \frac{V_\theta}{U},\ \bar{Z} = \frac{z}{L},\ \bar{r} = \frac{r}{r_o},\ \alpha = \frac{r_o}{r_i}, \quad (14)$$

where $\bar{V_z}$, $\bar{V_\theta}$, $\bar{Z}$, $\bar{r}$, and α are the dimensionless axial velocity, dimensionless swirl velocity, dimensionless axial coordinate, dimensionless radial coordinate, and radius ratio, respectively. The specific heat C_p, density ρ, dynamic viscosity μ, and Prandtl number Pr of the water as the working fluid were constant with values of 4178 J kg^{-1} K^{-1}, 996 kg m^{-3}, 0.798×10^{-3} kg m^{-1} s^{-1}, and 5.42 respectively. The outer radius of the annulus was r_o=20.05 mm, while the inner radius was r_i=15.93 mm, thereby forming an annular gap of 4.12 mm and a radius ratio of $\alpha = r_i/r_o$=0.8. The length of the annulus was equal to L=1500 mm. The boundary conditions are the no slip at the solid walls, uniform velocity and temperature profiles at the inlet and developed flow at the outlet. At the outlet boundary there is no information about the variables and some assumptions have to be made. The diffusion fluxes in the direction normal to the exit plane are assumed to be zero. The pressure at the outlet boundary is calculated from the assumption that radial velocity at the exit is neglected, so that the pressure gradient from r-momentum is given by:

$$\frac{\partial p}{\partial r} = \frac{\rho V_\theta^2}{r} \quad (15)$$

Due to memory limitations, axis-symmetric solutions were obtained. The center-line boundary was considered axis of symmetry. Uniform wall temperature (T_w=constant) as a thermal boundary condition is assumed for the inner wall. The outer wall is assumed to be perfectly insulated (q_w=0). For uniform wall temperature boundary condition, φ given by:

$$\varphi = \frac{T - T_w}{T_{in} - T_w} \quad (16)$$

where T_w is the inner wall temperature and T_{in} is the inlet fluid temperature. For the case of uniform inner wall temperature, the Nusselt number is given by:

$$Nu = \frac{h D_h}{k} = \frac{2(1-\alpha)}{\varphi_b} \frac{\partial \varphi}{\partial \bar{r}}\bigg|_{\bar{r}=\alpha} \quad (17)$$

where h is the heat transfer coefficient and

$$\varphi_b = \frac{T_b - T_w}{T_{in} - T_w} \quad (18)$$

is the dimensionless bulk temperature. The bulk temperature, T_b, is given by:

$$T_b = \int_{r_i}^{r_o} u T \, r\,dr \Big/ \int_{r_i}^{r_o} u\, r\,dr \quad (19)$$

Inlet boundaries for k and ε: The turbulence intensity, I, can be estimated from the following formula derived from an empirical correlation for pipe flows:

$$I = \frac{u'}{V} = 0.16(\mathrm{Re})^{-1/8} \quad (20)$$

An approximate relationship between the turbulence length scale, L_o, and the physical size of the annulus hydraulic diameter D_h is

$$L_o = 0.07 D_h \quad (21)$$

The relationship between the turbulent kinetic energy, k, and turbulence intensity, I, is

$$k = \frac{3}{2}(V\ I)^2 \quad (22)$$

The turbulence dissipation rate ε can be determined as

$$\varepsilon = C_\mu^{3/4} \frac{k^{3/2}}{L_o} \quad (23)$$

Wall boundaries for k and ε: In this study, the standard wall functions [24] are implemented. The boundary condition for k imposed at the wall is

$$\frac{\partial k}{\partial n} = 0 \quad (24)$$

where n is the local coordinate normal to the wall. The turbulence dissipation rate ε is computed from

$$\varepsilon = C_\mu^{3/4} K^{3/4} / \kappa y_p \quad (25)$$

where κ is von Kármán constant (= 0.4187), and y_p is distance from point p to the wall.

2.3 Solution Procedure

The governing equations for mass, momentum, energy, turbulent kinetic energy and its dissipation rate were solved using the control-volume method described by Patankar [25]. The convective and diffusive terms were discretized using power law scheme and the SIMPLER algorithm [25] was used to resolve the pressure-velocity coupling. For all the simulations performed in this study, converged solutions were usually achieved with residuals as low as 10^{-6} for all governing equations. The grid points are not distributed uniformly over the computational domain. They have greater density in the radial direction and have a lower density in the axial direction. The 2-D axisymmetric case with 300000 quadrilateral grid cells is chosen and an unstructured grid was used for the present simulation. The mesh is sufficiently refined in order to resolve the expected large flow parameter gradients. The under-relaxation parameters on the velocities were selected 0.3-0.5 for the radial and axial, and 0.9 for the swirl velocity components. Segregated, implicit solver has been applied through annulus. When using the present turbulent model it is necessary to run the simulation for a significant number of iterations, beyond normal convergence criteria. Experience has shown that typically 4000 iterations needed before the peak tangential velocity in the simulation stabilizes. In order to ensure the accuracy of the results and their independence with respect to the number of nodes used in the discretization process, several grids were tested. A grid independent solution study was made by performing the simulations for three different grids consisting of 250000, 300000, and 350000 nodes. A mesh refinement study showed a grid of 300000 nodes to be fine enough to capture all the flow features.

3 Results and Discussion

The problem of forced convection between two concentric horizontal cylinders is studied experimentally by Lu and Wang [17] for different Reynolds number. In order to gain confidence and understand the modeling methodology that is required to adequately simulate the heat transfer in the annulus, the experimental work of Lu and Wang [17] is used as a case study to validate the modeling approach presented in this paper. Computations were firstly performed for this geometry without swirl to validate the accuracy of the numerical results by comparing with the experimental results. Table 1 compares the predicted and the measured average Nusselt numbers for different Reynolds numbers, the mean Nusselt number is obtained by integrating the local Nusselt number over the inner cylinder. The result presented in Table 1 for Reynolds number ranging from 5000 to 10000. Results are shown in Table 1 represent good agreement between the present computations and experiments of Lu and Wang [17]. The predicted values of Nusselt numbers compare well with the measured values with maximum percentage error less than 5%.

Table 1: The comparison between predicted and experimental data of average Nusselt numbers

Re	$Nu_{m,\ experiment}$	$Nu_{m,\ present\ simulation}$	% error
4000	43	45.15	4.7
5000	57	55.14	3.3
8000	87	89.32	2.7
10000	105	108.25	3.1

The characteristics of the swirling flow and forced convective heat transfer on the conditions of developed turbulent flow in narrow annuli are now presented and discussed. The solutions were carried out for different inlet swirl numbers S. The entrance length effect can be neglected; the flow is hydrodynamically fully developed and somewhat flatter in turbulent flow as expected. The strength of vortex flow has a great influence on the axial velocity profile. Fig. 2 shows the developed axial velocity profiles in the annulus in turbulent flow, Re=5000, for inlet swirl number of S=0, 2 and 3. It can be seen from Fig. 2 and that when the

inlet swirl number increases it increases the axial velocity near the wall and reduces it at the mid-gap to achieve the conservation of mass due to the existence of the recirculation zone, eddy motion, mixing in radial direction and centrifugal forces. Fig. 3 shows the development of the non-dimensional swirl velocity in the annulus in turbulent flow at different axial positions $\bar{Z}$ =0.07, 0.13, 0.33, 0.5, 0.67, and 0.87. In general, at specified inlet swirl number and Reynolds number, as an example S=2 and R_e = 5000, the swirl velocity profiles decay along the annulus due to viscous effects at the wall which leads to damp the tangential velocity. The maximum tangential velocity does not occur at the mid-gap but occurs close to the outer wall, especially for the entrance region due to strong centrifugal force. The local Nusselt number at the lower wall for the horizontal flow in the annulus for turbulent flow is simulated and plotted for different inlet swirl numbers in Fig. 4. Simulations show that the inlet swirl numbers have great influences on the heat transfer characteristics. The variation of local Nusselt number along the annulus in turbulent flow, thermally developed flow, for uniform surface temperature is given in Fig. 4, the local Nusselt number was plotted as a function of the dimensionless axial location $\bar{Z}$ for Re=5000 and for the range of swirl numbers of S=0, 2 and 3. The Nusselt number decreased approximately up to ten annulus hydraulic diameters, and then it remained nearly constant at specified inlet swirl number because of the thermally developed flow. The last figure indicated that the Nusselt number of turbulent flow in the annulus with swirl is higher than that without swirl for the same Reynolds numbers. The enhancement in the local Nusselt numbers compared to values obtained in the axial flow was higher at higher swirl number because of the higher swirl intensity. The centrifugal force results in the development of secondary flows which help in mixing the fluid and enhance the heat transfer. In addition, the Nusselt numbers and thus the convection heat transfer coefficients are much higher in the entrance region. It can be also observed that as the swirl number increases, the Nusselt number increases. This behavior is related to the wall velocity gradient, which increase with the widening of the axial velocity around the mid-gap. In early work [6] the existence of the recirculation zone has been mentioned as a possible mechanism of heat transfer enhancement in the swirl flows. Indeed, the recirculation zone improves the convective heat transfer because it increases the axial velocity near the wall. The increase of the near-wall velocity, in turn, produces larger temperature gradients and higher heat transfer rate. It was shown experimentally [26] that one of the major mechanisms of the heat transfer enhancement is a high axial velocity near the wall. For swirling flow, the local Nusselt number decayed along the annulus in the axial direction as the axial distance increased, but the effect of swirl was still considerably evident at the end of the annulus. As the fluid flows along the annulus, the angular momentum and tangential velocity decay due to friction losses at the wall. Some investigators, including Baker and Sayre [27] and Kreith and Sonju [28], observed that the decay process showed an exponential behavior.

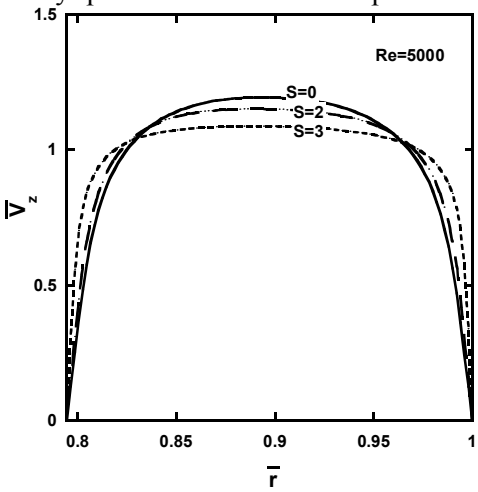

Fig. 2: The axial velocity profiles in the annulus in turbulent flow at different swirl numbers

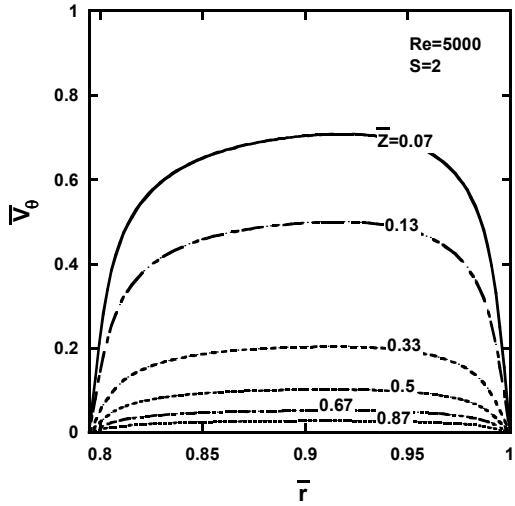

Fig. 3: Swirl velocity profiles in the annulus in turbulent flow

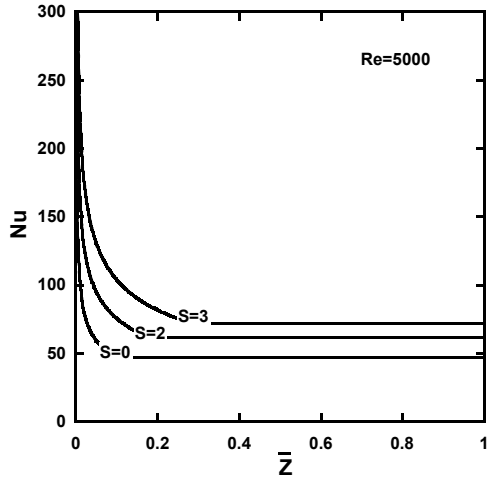

Fig.4: Variation of local Nusselt number along annulus in turbulent flow for uniform surface temperature

4 Conclusions

The characteristics of the turbulent swirling flow and convective heat transfer on the in narrow annular were solved by means of a finite volume technique. The predicted average Nusselt numbers were found to be in good agreement with experimental data. Simulations in the present studies revealed that the inlet swirl number has great influences on the heat transfer characteristics. Nusselt numbers were seen to increase with imposing swirl to the entrance of the annulus. When the inlet swirl number increases it increases the axial velocity near the wall and reduces it at the mid-gap due to centrifugal forces. The increase of the near-wall velocity produces larger temperature gradients and higher heat transfer rate. The swirl velocity profiles decay along the annulus as a result of wall friction which leads to damp the swirl velocity.

References:

[1] R.K. Shah, A.L. London, Laminar Flow Forced Convection in Ducts, Advances in Heat Transfer, Academic Press, New York, 1978.

[2] S. Kakac, R.K. Shah, W. Aung, Handbook of Single-Phase Convective Heat Transfer, John Wiley, New York; 1987.

[3] Yunus A. Cengel, Heat and Mass Transfer, A practical Approach**,** 3rd Ed., McGraw Hills Inc., USA; 2006.

[4] AK. Gupta, DG. Lilley, N. Syred, Swirl flows, Ohu: Abacus Press; 1984.

[5] F. Kreith, MS Bohn, Principles of heat transfer, St. Paul: West Publishing Company; 1993.

[6] R. Razgaitis, JP. Holman, A survey of heat transfer in confined swirl flows, Heat Mass Transfer Processes, 1976; 2:831–66.

[7] T.H. Kuhen and R.J. Goldstein, An experimental and theoretical study of natural convection in the annulus between horizontal concentric cylinders, J. Fluid Mech., 74, 1979, 695-719.

[8] A.M. Jawarneh, P. Sakaris , and G.H. Vatistas, Experimental and analytical study of the pressure drop across a double-outlet vortex chamber, Transaction of ASME, Journal of Fluids Engineering**,** Vol. 129, issue 1, 2007, 100-105.

[9] A.M. Jawarneh, G.H. Vatistas G.H. and H. Hong, On the flow development in jet-driven vortex chambers, AIAA, Journal of Propulsion and Power, Vol. 21, No. 3, 2005, 564-570.

[10] M. Yilmaz, S. Yapici, O. Jomakli, and O.N. Sara, Energy correlation of heat transfer and enhancement efficiency in decaying swirl flow, Heat Mass Transfer, 38, 2002, 351-358.

[11] S. Martemianov, V.L. Okulov, On heat transfer enhancement in swirl pipe flows, Int. J. of heat and Mass Transfer, 47 (2004), 2379-2393.

[12] H.Y Zeng, S.Z Qiu, D.N Jia, Investigation on the characteristics of the flow and heat transfer in bilaterally heated annuli, Int. J. of Heat and Mass Transfer 50 (2007) 492-501.

[13] E.K. Akpinar, Y. Bicer, C. Yildiz, and D. Pehlivan, Heat Transfer Enhancement in a concentric double pipe exchanger equipped with swirl element, Int. Comm. Heat Mass Transfer, Vol. 31, No. 6, 2004, 857-868.

[14] S.A. Berger, L. Talbot, L.S. Yao, Flow in curved pipes, Annual Review of Fluid Mechanics 15 (1983) 461–512.

[15] L.A.M. Janssen, C.J. Hoogendoorn, Laminar convective heat transfer in helical coiled tubes, International Journal of Heat and Mass Transfer 21 (1978) 1197–1206.

[16] D.G. Prabhanjan, G.S.V. Raghavan, T.J. Rennie, Comparison of heat transfer rates between a straight tube heat exchanger and a helically coiled heat exchanger, International Communications in Heat and Mass Transfer 29 (2) (2002) 185–191.

[17] G. Lu, J. Wang, Experimental investigation on heat transfer characteristics of water flow in a narrow annulus, Applied Thermal Engineering xxx (2007) xxx–xxx. *In Press, Corrected Proof, Available online 20 March 2007*

[18] J. Dirker, J.P. Meyer, Heat transfer coefficients in concentric annuli, Journal of Heat Transfer 124 (2002) 1200–1203.

[19] Ichimiya, Koichi, Hasegawa, Enhancement forced convective heat transfer in narrow concentric annulus by turbulence promoters, Journal of the Atomic Energy Society of Japan 26 (8) (1984) 698–707.

[20] T.J. Rennie, V.G.S. Raghavan, Experimental studies of a double-pipe helical heat exchanger, Experimental Thermal and Fluid Science 29 (2005) 919–924.

[21] D. Mateescu, M.P. Paidoussis, Unsteady viscous effects on the annular-flow-induced instabilities of a rigid cylinder body in a narrow duct, J. of Fluid and Structures 1, 1987, 197-215.

[22] T.H. Chang, Experimental study on turbulent swirling flow in a cylindrical annuli by using the PIV technique, International Journal of Automotive Technology, Vol. 5, No. 1, 2004, 17−22.

[23] R. De Parias Neto, P. Legentilhomme, and J. Legrand, Finite-element simulation of laminar swirling decaying flow induced by means of a tangential inlet in an annulus, Computer Methods in Applied Mechanics and Engineering, Vol. 165, 1998, 189-213.

[24] B. E. Launder and D. B. Spalding, The Numerical Computation of Turbulent Flows, Computer Methods in Applied Mechanics and Engineering, 1974, 3:269-289.

[25] V. Patankar, Numerical Heat Transfer and Fluid Flow, Hemisphere, New York, 1980.

[26] F. Chang, V.K. Dhir, Mechanisms of heat transfer enhancement and slow decay of swirl in tubes using tangential injection, Int. J. Heat Fluid Flow 16 (2) (1995) 78–87.

[27] DW Baker, Sayre Jr CL. In: Dowdell RB, editor. Proceedings of Symposium on Flow: Its Measurement and Control in Science and Industry, vol. 1, 1974. p. 301–312.

[28] F Kreith, OK Sonju, The decay of a turbulent swirl in a pipe. J Fluid Mech 1965;22:257–71.